

Bed-load transport for steady flows and unsteady oscillatory flows

Jan S. Ribberink

University of Twente, Faculty of Technology and Management, Department of Civil Engineering, P.O. Box 217, 7500 AE Enschede, The Netherlands. j.s.ribberink@sms.utwente.nl

Received 22 August 1997; revised 8 January 1998; accepted 19 February 1998

Abstract

The validity of a bed-load transport formula, based on the bed-shear concept of Meyer-Peter and Mueller, was investigated for steady unidirectional flows, oscillatory flows and oscillatory flows with superimposed net currents. The aim of the study was to develop a general bed-load transport concept for a wide range of flow and sediment conditions, as occurring in the marine coastal environment. The results of more than 150 laboratory experiments, including more than 75 recent bed-load transport measurements in oscillating water tunnels, were used for the study. For oscillatory flows, the time-dependent bed-load transport was treated in a ‘quasi-steady’ way and an equivalent Shields parameter θ'_{eq} was defined in order to enable a comparison between ‘steady flow’ and ‘unsteady oscillatory flow’ measurements. A good correlation was found between the non-dimensional transport parameter Φ_b and the non-dimensional excess bed-shear $\theta'_{eq} - \theta_c$ for different sets of oscillatory bed-load transport measurements. However, especially in the lower Shields regime, the oscillatory flow data show a clear deviation from an extensive set of steady flow bed-load data. A good agreement between the (oscillatory flow and the steady flow) data sets could then be obtained by reducing the lower limit of the roughness height k_s for oscillatory flows from the (steady flow) value $3D_{90}$ to D_{50} . Based on the obtained concept a generalized bed-load formula was derived for both flow types, including oscillatory flows and superimposed currents under an arbitrary angle. A verification, carried out with a set of (co-linear) oscillatory + superimposed current measurements, showed a good agreement between calculated and measured bed-load transport rates. Finally, the validity and limitations of the obtained bed-load model are discussed. © 1998 Elsevier Science B.V. All rights reserved.

Keywords: Sand transport; Bed-load transport; Waves; Hydraulics

1. Introduction

Accurate prediction of sediment transport rates is generally an important element in morphological studies in river and coastal marine environments. The earliest, basically

empirical, formulas were developed a few decades ago for steady uniform flows (Meyer-Peter and Mueller, 1948; Einstein, 1950; Engelund and Hansen, 1967). These formulas, which are still widely used for river applications, are all based on the concept that the sediment transport rate can be related to the shear stress exerted on the bed by the fluid above (bed-shear stress concept).

In the marine coastal environment, the process of sediment transport becomes increasingly complex due to the presence of different types of unsteady flows, as caused by tidal influence and wind waves. Different lines of sediment transport research and model development are followed to cope with coastal flows, leading to various model concepts for various types of sediment transport in the coastal zone. The longshore transport is generally modelled at an intra-wave time scale, as far as tidal flow is concerned, but at a wave-averaged time scale for the short wind waves (Bijker, 1967; van Rijn, 1993). The sediment stirring influence of the short waves is expressed in an increased bed-shear stress and an increased vertical mixing coefficient (diffusion) for the sediment in suspension.

For the cross-shore sediment transport, a wave-averaged approach is not adequate, due to the dominant role of the time-dependent oscillatory orbital motion near the sea bed, as induced by the short waves. For example, the residual cross-shore transport of sand due to short-wave asymmetry is generally tackled with an intra-wave model concept, describing the unsteady transport process through the wave cycle. Bagnold (1956, 1963) developed an 'energetics transport model concept', in which the instantaneous transport through the wave cycle is related to the instantaneous energy dissipation rate due to bottom friction. Bagnold's concept formed the basis for the bed-load transport models of Bailard and Inman (1981) and the total load transport model of Bailard (1981). Madsen and Grant (1976) used the 'bed-shear stress concept' for river flow of Einstein (1950) as the basis for a transport formula for cross-shore transport. In Bagnold's as well as Madsen and Grant's modelling concepts the time-dependent transport through the wave cycle is treated in a quasi-steady way, i.e., unsteady effects such as time-history effects from previous phases of the wave cycle or from previous wave cycles are neglected. Basically, in both concepts, the time-dependent transport through the wave cycle is related to (some power of) the horizontal oscillatory flow velocity directly above the wave boundary layer.

Also more refined mathematical modelling attempts were made during the last decades in order to describe the near-bed transport processes, taking place in and directly above the wave boundary layer (Bakker, 1974; Smith, 1977; Fredsøe et al., 1985). This has led to suspension models with sophisticated turbulence closures (see Davies, 1990; Davies et al., 1996), two-phase flow models for sheet flow (Asano, 1990) and, e.g., discrete vortex models for rippled beds (Hansen et al., 1994). Despite these efforts, the present state of knowledge of the dynamics of sediment transport still does not allow a full dynamic description of the sediment/water flows based on first principles. The development of practical sediment transport models still has a strong empirical character and relies heavily on physical insights and quantitative data as obtained in laboratory and field studies. Further development of models is generally hampered by the limited number of relevant and accurate laboratory and field data on near-bed transport processes.

Since 1990, a series of new laboratory datasets with measured sediment transport rates in full-scale wave-induced oscillatory flows became available, as a result of a continuing experimental research programme in a Large Oscillating Water Tunnel (Al-Salem, 1993; Ribberink and Al-Salem, 1994; Ribberink et al., 1994). These experiments were carried out on realistic (prototype) scales, generally using common beach sand (0.2 mm median grain size) and covering a wide range of random/regular oscillatory flows and superimposed net currents.

In the present paper, the new data and the physical insights, as obtained from these measurements, are used for the development of a semi-empirical bed-load transport formulation for steady currents, waves and combined wave-current flows. The objective of the study is to develop a general formulation for the prediction of bed-load transport in a wide range of river and coastal conditions. Apart from the new data also (recent and older) steady and unsteady flow/sediment transport data from various other sources are used for the model development.

2. Bed-load transport modelling

Although a distinction between bed-load transport and suspended-load transport is generally made and widely accepted, the definition of both transport modes is not fully clear. The rolling, sliding and jumping grains in almost continuous contact with the bed, are generally referred to as bed-load. Intergranular collision forces play an important role. Grains which are almost continuously suspended in the water column during their transportation and which are dominated by the turbulence mixing processes without important intergranular collisions, are generally referred to as suspended load. Sheet flow is an intermediate transport mode in which a layer with a thickness of several grain layers (10–100) and large sediment concentrations ($> \text{ca. } 5\text{--}10 \text{ vol.}\%$) is transported along the bed. Grains in this high-concentration layer do not only roll or slide over the non-moving bed surface, but intergranular contact between moving grains and extra pressure forces due to grain–water interactions become important also. Following the ideas of Wilson (1987), in the present study, sheet flow is considered as being part of the bed-load transport.

‘Quasi-steady’ modelling of the intra-wave transport process is especially questionable for suspended sediment, e.g., in the surf zone with breaking waves, due to the adjustment time needed for resuspension and settling. Also in the case that vortex ripples are present on the sea bed, coherent sediment clouds (vortices) can be suspended up to elevations of several ripple heights above the bed and the assumption of quasi-steadiness is strongly violated (see, e.g., Sato, 1987; Villaret and Perrier, 1992). In the higher flow regimes with flat sea beds and sheet flow, the stirring capacity of the oscillatory flow is considerably reduced, due to the absence of the large coherent vortex motions and due to turbulence damping effects (flow stratification; see Ribberink and Al-Salem, 1994).

Horikawa et al. (1982), Ribberink and Al-Salem (1994) and Ribberink et al. (1994) show for a range of different oscillatory sheet flows (with and without superimposed net currents) that 90–100% of the time-dependent and time-averaged sediment flux is concentrated in a thin sheet flow layer with a thickness of order millimetres. Due to this

small transport layer thickness the periodic pick-up and settling process of grains through the wave cycle takes place at a time-scale (fractions of a second) which is much smaller than the period of sea waves (5–15 s). Fig. 1 shows a typical example of measured time-dependent concentrations in an oscillatory sheet flow layer in the case of a sinusoidal flow (velocity amplitude $\hat{U} = 1.7$ m/s, period $T = 7.2$ s) and 0.21 mm sand (median grain size). In the lower bed layers or pick-up layer ($z < 0$ mm) as well as in

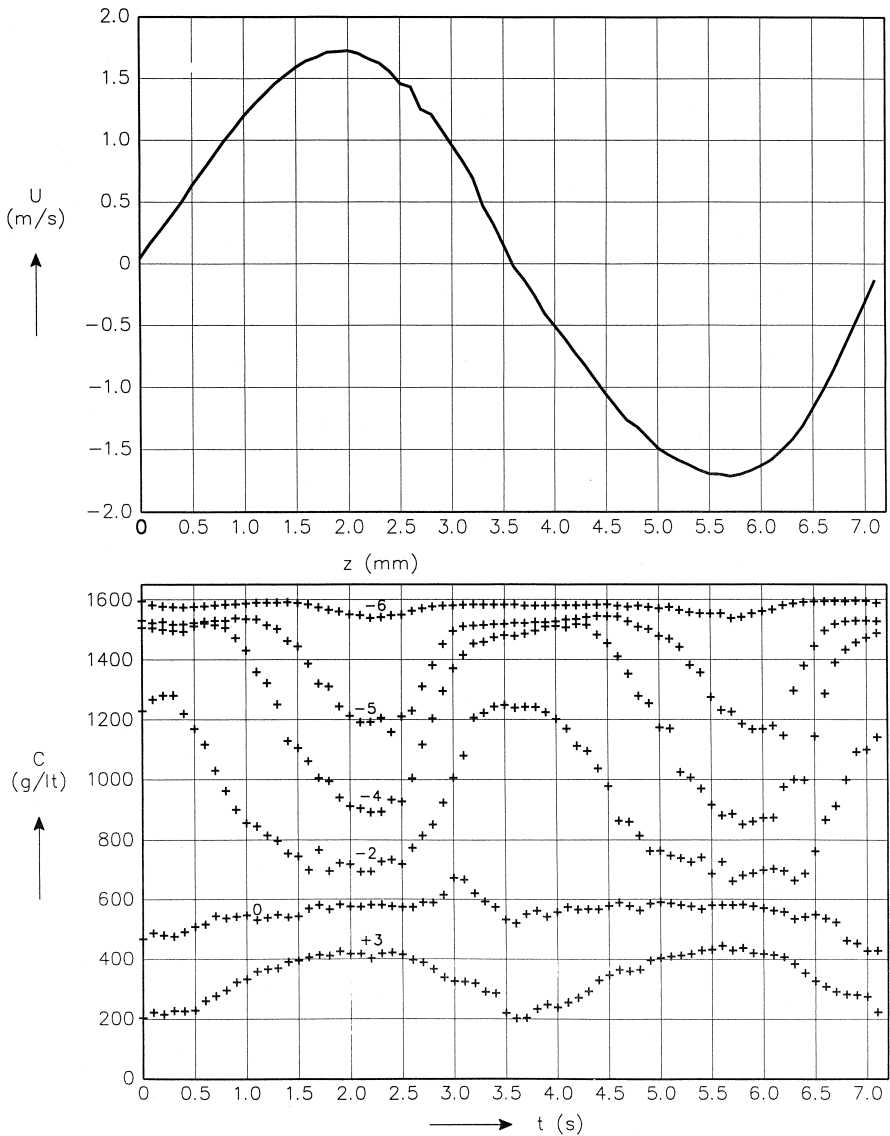


Fig. 1. Time-dependent concentrations in the sheet flow layer (lower plot) for sinusoidal oscillatory flow (upper plot); elevation $z = 0$ corresponds with the bed level in the case of no sediment motion.

the upper sheet flow layer ($z > 0$ mm), the time-dependent concentration shows only minor phase lags in comparison to the horizontal oscillatory flow velocity above the wave boundary layer. Ribberink and Al-Salem (1994) show that due to this quasi-steady behaviour without important time-history effects, the net (time-averaged) sediment transport rate $\langle q_s \rangle$ can be expressed reasonably well in terms of the time-dependent flow velocity $U(t)$ alone. Fig. 2 shows the good correlation between measured net transport rates $\langle q_s \rangle$ and the 3rd-order velocity moment $\langle U^3 \rangle$ as was found for a wide range of asymmetric (2nd-order Stokes) waves and wave-current combinations with 0.21 mm sand (Ribberink et al., 1994).

These insights into the oscillatory sheet flow process form the basis of the present work, in which an attempt is made to develop a quasi-steady bed-load transport formula in a (semi-) empirical way, using a large dataset of laboratory and field measurements. The study is aimed at finding a general concept in which the connection is made between waves and steady flows, in the low-velocity regime (e.g., tidal and river flow) as well as in the high-velocity regime (e.g., wave-induced sheet flow).

A number of classical non-dimensional parameters are used. The bed-load transport is represented as:

$$\Phi_b = \frac{q_b}{\sqrt{\Delta g D_{50}^3}} \quad (1)$$

in which: q_b = bed-load transport rate in volume per unit time and width; D_{50} = median grain diameter; Δ = relative density = $(\rho_s - \rho)/\rho$; ρ_s = density of sand; ρ = density of water; g = gravity acceleration.

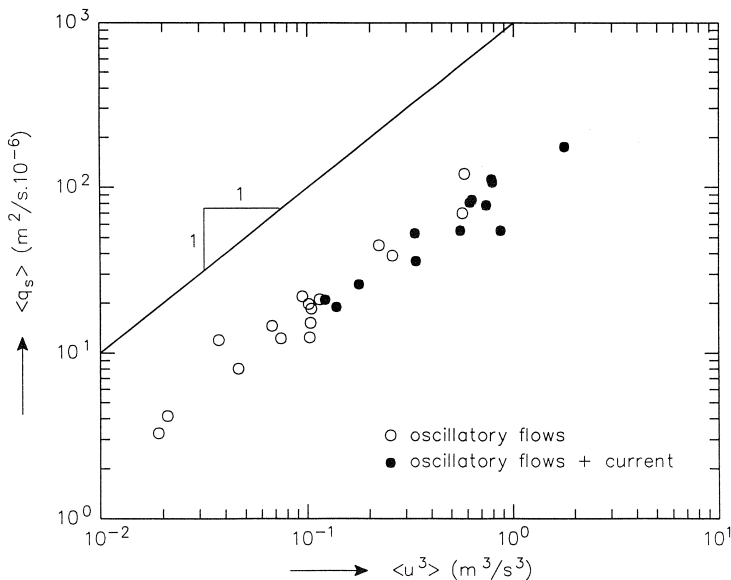


Fig. 2. Net sand transport rate vs. the 3rd-order velocity moment for oscillatory flow experiments in the oscillating water tunnel with and without a superimposed net current ($D_{50} = 0.21$ mm sand).

The Shields parameter is used as non-dimensional sediment forcing parameter:

$$\theta = \frac{\tau_b}{(\rho_s - \rho) g D_{50}} \quad (2)$$

in which: τ_b = bed-shear stress.

A threshold of motion for sand grains is included by using the critical Shields parameter θ_c , which is described as a function of the non-dimensional grain size D_* , as follows (van Rijn, 1993):

$$\begin{aligned} \theta_c &= \frac{\tau_{b_c}}{(\rho_s - \rho) g D_{50}} \\ &= 0.24 D_*^{-1} && \text{for } 1 < D_* < 4 \\ &= 0.14 D_*^{-0.64} && \text{for } 4 < D_* < 10 \\ &= 0.04 D_*^{-0.1} && \text{for } 10 < D_* < 20 \\ &= 0.013 D_*^{0.29} && \text{for } 20 < D_* < 150 \\ &= 0.055 && \text{for } D_* > 150 \end{aligned} \quad (3)$$

in which:

$$D_* = D_{50} \left(\frac{g \Delta}{\nu^2} \right)^{\frac{1}{3}} \quad (4)$$

with: τ_{b_c} = critical bed-shear stress; ν = kinematic viscosity of water.

In the following, steady flow conditions (currents) are considered first, and a bed-load model concept is verified with different sets of existing laboratory and field data, covering a wide range of grain mobility conditions ($\theta_c < \theta < 10$). The model concept is then verified and improved for unsteady oscillatory flow conditions, using a number of datasets from recent experiments in oscillating water tunnels. Finally, the formulation is generalized for oscillatory flows with superimposed net currents and verified with a series of co-linear oscillatory flow/net current data.

3. Steady flows

For steady flows, a non-dimensional bed-load formula of the shape:

$$\begin{aligned} \Phi_b &= m \{ \theta' - \theta_c \}^n && \text{for } \theta' \geq \theta_c \\ &= 0 && \text{for } \theta' < \theta_c \end{aligned} \quad (5)$$

is commonly accepted. An effective Shields parameter θ' represents that part of the total bed-shear which is used for the bed-load transport process. The remaining part θ'' ($= \theta - \theta'$) is used to overcome the drag force (per unit bed area) exerted on bedforms. Meyer-Peter and Mueller (1948) derived this type of equation on the basis of flume experiments with rather coarse sand ($D > 3$ mm) and for low Shields numbers ($\theta < 0.2$). They obtained the values $n = 1.5$ and $m = 8$ in Eq. (5). Fernandez Luque and van Beek (1976) performed experiments with smaller grain sizes ($D > 0.9$ mm) for rather low

Shields numbers ($\theta < 0.1$) and found $n = 1.5$ and $m = 5.7$. Wilson (1987) provided a theoretical basis for this type of formula in sheet flow conditions ($\theta > 1$). Nnadi and Wilson (1992) published laboratory experiments of Wilson (1966) which were carried out in a duct for very high Shields numbers (sheet flow regime, $\theta > 1$) and one grain size ($D = 0.7$ mm). According to these data $n = 1.5$ and $m = 12$.

For steady uniform flows, the effective Shields parameter can be based on the depth-averaged current–velocity V and can be computed as follows:

$$\theta' = \frac{\tau_b}{(\rho_s - \rho) g D_{50}} \quad (6)$$

with:

$$\tau_b = \rho g \frac{V^2}{C'} \quad (7)$$

The Chézy friction coefficient C' is based on the skin friction of the bed, using a rough-wall friction formulation and a Nikuradse grain-roughness height k_s :

$$C' = 18 \log \left(\frac{12h}{k_s} \right) \quad (8)$$

in which: C' = Chézy friction coefficient based on grain roughness (skin friction); h = water depth; k_s = roughness height.

The following alternative formulation for the bed shear stress can be used in the case of a prescribed near-bed velocity at an arbitrary level $z = \delta$ above the bed in the logarithmic layer ($u_b = u_b(\delta)$):

$$\tau_b = \frac{1}{2} \rho f'_c u_b^2 \quad (9)$$

$$f'_c = 2 \left(\frac{0.4}{\frac{\delta}{z_0}} \right) \quad (10)$$

with:

$$z_0 = \frac{k_s}{30}$$

Contrary to the ‘depth-averaged’ Eqs. (7) and (8), which are based on the assumption of a logarithmic velocity profile shape along the whole water column, Eqs. (9) and (10) assume a log-profile only near the bed ($z < \delta$). This ‘near-bed’ approach has a more general validity than the ‘depth-averaged’ approach, since non-uniform and/or non-steady flows are not necessarily excluded.

The characteristic (Nikuradse) grain roughness height k_s is proportional to a characteristic grain size. Based on the analysis of various sets of experiments, van Rijn concludes that the grain roughness is mainly related to the largest particles of the top layer of the bed (see van Rijn, 1982). He proposes for low Shields numbers:

$$k_s = 3 D_{90} \quad \text{for: } \theta' < 1 \quad (11)$$

Table 1
Steady flow laboratory experiments

Author	Experimental facility	D_{50} (mm)	Number of experiments	Range of θ'
Guy et al. (1966)	flume	0.19	12	0.07–1.1
		0.28	17	0.1–1.1
		0.45	3	0.1–0.4
		0.93	16	0.07–0.3
Nnadi and Wilson (1992)	duct	0.70	45	0.8–7.7

Wilson (1989) argues that flat mobile beds at high shear stresses (sheet flow, $\theta = \theta' > 1$) can neither be considered as a rough or smooth (fixed) wall but they obey their own friction law with a frictional length scale proportional to the thickness δ of the sheet flow layer. He shows that the sheet flow behaviour can be made formally equivalent to the rough wall case, by setting the roughness height k_s to a multiple of δ ($k_s \approx 0.5\delta$). As δ itself is proportional to the Shields parameter θ , this leads to an implicit relation for k_s . Based on a large set of bed-shear stress measurements in a closed conduit with sand and nylon particles, Wilson suggest $k_s = 5\theta D_{50}$ for high

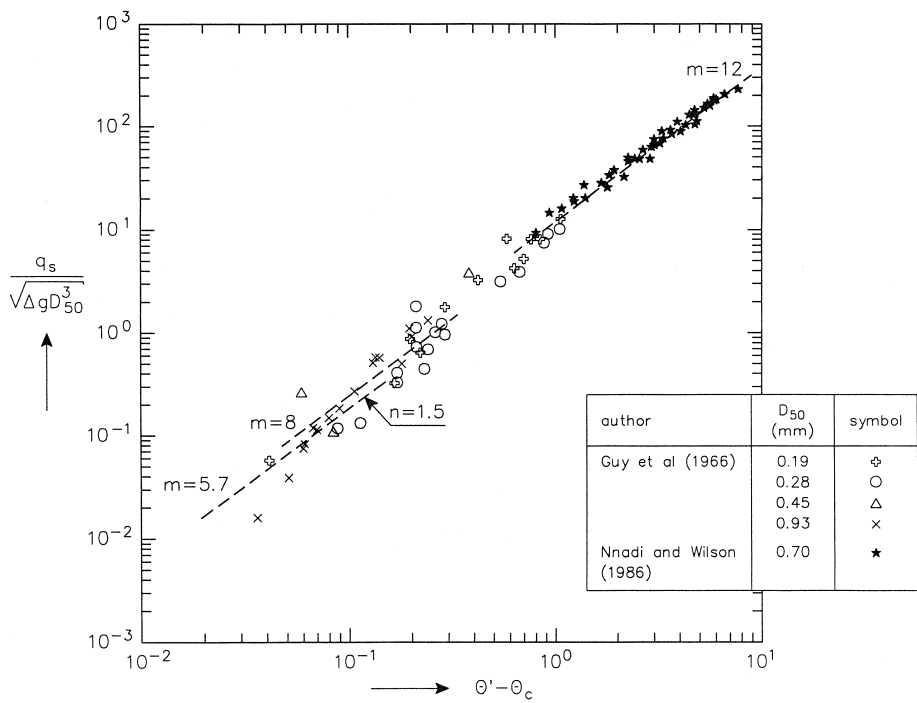


Fig. 3. Steady flows: measured dimensionless sand transport rates vs. the effective Shields parameter minus the critical Shields parameter (excess bed-shear) and the power formulas of Fernandez Luque and van Beek ($m = 5.7$), Meyer-Peter and Mueller ($m = 8$) and Nnadi and Wilson ($m = 12$).

Shields numbers in the range $1 < \theta < 7$. A closer focus on the sand data suggests the following slightly different relation:

$$k_s = D_{50} [1 + 6(\theta - 1)] \quad \text{for: } \theta > 1 \quad (12)$$

In the present study, Eqs. (11) and (12) are both used in the sense that the maximum predicted value of both expressions is used for the bed-shear stress calculation:

$$k_s = \max \{3D_{90}, D_{50} [1 + 6(\theta - 1)]\} \quad (13)$$

The complete bed-load transport model concept (Eqs. (5)–(13)) is verified for a wide range of steady flow conditions, using the laboratory data of Guy et al. (1966), with Shields numbers generally $\theta < 1$, and the sheet flow data of Nnadi and Wilson (1992) with generally $\theta > 1$. It should be mentioned that during most of the flume experiments of Guy et al. (1966) bedforms were present, while during Wilson's duct experiments (Nnadi and Wilson, 1992) the bed was completely flat. Moreover, in the latter experiments all sediment is transported as contact load or sheet flow (see Wilson, 1966, 1987). The data of Guy et al. are obtained from van Rijn (1981), who calculated the bed-load transport rates during these flume tests from the measured total and suspended transport rates. Table 1 summarizes the conditions of these experimental datasets, i.e.,

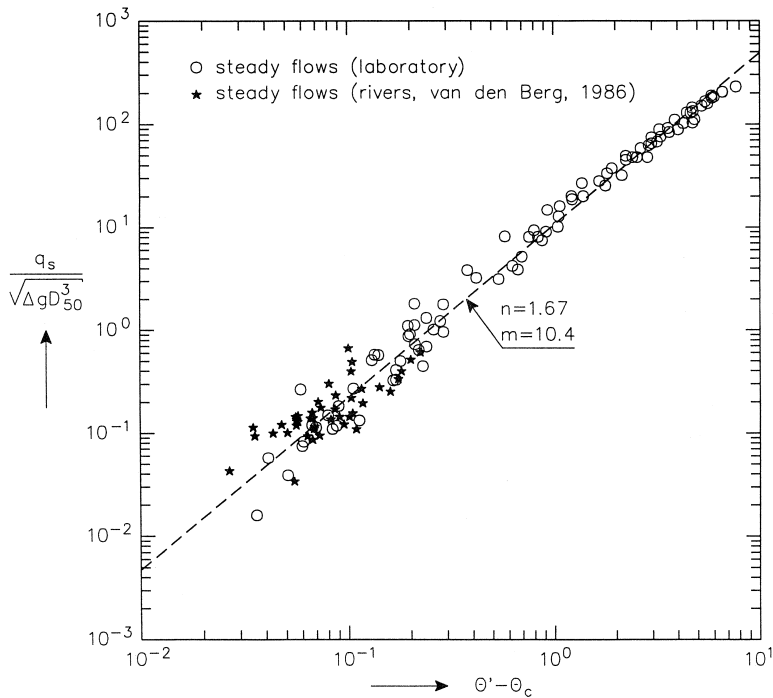


Fig. 4. Steady laboratory and river flows: measured dimensionless sand transport rates vs. the effective Shields parameter minus the critical Shields parameter (excess bed-shear) and a fitted power formula for the full data range ($m = 10.4$, $n = 1.67$).

Table 2
River data (after van den Berg, 1986)

River	D_{50} (mm)	Number of measurements	Range of θ'
Rhine	3.6	3	≈ 0.1
Pannerden Channel	3.8	8	0.08–0.10
Waal	1.05	6	0.17–0.25
Waal	0.95	5	0.12–0.15
IJssel	0.69	3	≈ 0.1
Hii	1.44	4	0.09–0.14
Hii	1.11	4	0.11–0.14
Skive Karup	0.46	1	≈ 0.12
Dommel	0.37–0.51	10	0.03–0.14

experimental facility, range of grain sizes, number of experiments and the range of Shields values.

The performance of the bed-load formula is shown in Fig. 3 by plotting the measured dimensionless bed-load transport Φ_{bd} against the excess (dimensionless) bed-shear stress $\theta' - \theta'_c$ for the selected data of Table 1. The formulas of Fernandez Luque ($m = 5.7$), Meyer-Peter and Mueller ($m = 8$) and Nnadi and Wilson ($m = 12$) are also shown in Fig. 3 in their approximate range of validity ($n = 1.5$ for all three formulas). The overall correlation of the data is rather good, which reconfirms the validity of this (classical) bed-load transport formula. The scatter in the data of Guy et al. (1966) can probably be explained to some extent by inaccuracies in the measurement of the suspended sediment transport rate, the latter being subtracted from the total transport rate to determine the bed-load transport rate.

In Fig. 4, the laboratory data are plotted together with a set of river data, as published by van den Berg (1986) and summarized in Table 2. It is shown that the river data, which only cover the low flow regime ($\theta' < 0.3$), show a good agreement with the laboratory data.

A power function of the form of Eq. (5) is fitted through the datapoints, using the coefficients m and n as fit parameters. Due to the log scales, this function can be represented as a straight line in Fig. 4. The regression technique yields the following coefficients:

$$m = 10.4, \quad n = 1.67 \quad (14)$$

4. Oscillatory flows

For oscillatory flows, the bed-load Eq. (5) may be applied instantaneously at each phase of the wave cycle, assuming that the instantaneous bed-load transport can be directly coupled to the instantaneous bed-shear stress or near-bed horizontal orbital velocity at the same phase of the cycle. Time-dependent sediment flow phenomena,

taking place at the time scale of the wave period, can violate this assumption of quasi-steadiness and should therefore be negligibly small. These time-history effects could, for example, be related to, (i) delayed grain pick-up and acceleration (e.g., inertial effects for heavy and coarse sediments), (ii) delayed settling of grains (especially for light and fine sediments), and (iii) turbulence bursting processes with time scales of the order of the wave period.

During the past decade a series of new experimental datasets have become available with sediment transport measurements under the influence of oscillatory flows. A limited number of detailed experimental studies in oscillating water tunnels, carried out with fine sand (0.13 mm; King, 1991; Ribberink and Chen, 1993) and light-weight materials (Dick and Sleath, 1992) indeed show substantial time-dependent effects related to turbulent bursting processes. For example, Ribberink and Chen (1993) observe a strong reduction and even negative net transport rates in the case of a second-order Stokes asymmetric oscillatory (sheet) flow over a flat bed consisting of 0.13 mm sand (negative = in opposite direction as the peak velocity). Quasi-steady bed-load modelling is not appropriate in these conditions and these data as well as experimental data with very small wave periods—which are outside the range of relevant field conditions ($T \leq 3$ s)—are therefore not included in the present data analysis. For a better understanding and for improved modelling of these phenomena, additional experimental research is necessary (see Janssen and Ribberink, 1996; Janssen et al., 1997).

A large number of experimental studies, carried out with coarser sands ($D_{50} \geq 0.2$ mm), do confirm the quasi-steady nature of the oscillatory bed-load process. Horikawa et al. (1982), Staub et al. (1984), Sawamoto and Yamashita (1986), and Ribberink and Al-Salem (1995) presented detailed boundary layer measurements in various conditions, which show that near-bed sediment concentration and oscillatory flow velocities are closely coupled in time without important phase-lags (see Fig. 1).

Table 3 gives an overview of experimental studies that are used in the present study for the development of a quasi-steady bed-load model. The experiments were all conducted in oscillating water tunnels (OWT) for a wide range of Shields values (including the sheet flow regime), using sand with grain sizes in the range 0.2–1.8 mm. Net bed-load transport rates were measured for half sinusoidal wave cycles and full

Table 3
Data sets (oscillatory flows)

Author	Experimental facility	D_{50} (mm)	Full/ half cycle	Number of experiments	Range of θ'_{eq}
Ribberink and Al-Salem (1992)(series B)	OWT–DelftHydraulics	0.21	full	16	0.35–1.1
King (1991)	OWT–Scripps	0.44	half	21	0.11–0.75
Sawamoto and Yamashita(1996)	OWT–Tohoku University	1.10		11	0.1–0.4
		0.20	half	5	0.6–1.57
		0.70		5	0.27–0.61
		1.80		5	0.16–0.35

asymmetric (2nd-order Stokes) waves. During all experiments the bed was flat, i.e., bedforms (wave ripples) did not appear (Ribberink and Al-Salem, 1992) or bedforms did not have the time to be formed, due to the short experimental run times (King, 1991; Sawamoto and Yamashita, 1986). Ribberink et al. (1994) show that in this type of oscillatory sheet flow conditions 90–100% of the sediment flux is concentrated in a near-bed layer in the sheet flow layer with a thickness of about 1 cm where sediment volume concentrations range between 5% and 50–60%.

In order to cope with oscillatory flows the bed-load transport is described by Eq. (5) in the following time-dependent (intra-wave) form, which enables a sign change during the wave cycle:

$$\begin{aligned}\Phi_b(t) &= m(|\theta'(t)| - \theta_c)^n \cdot \frac{\theta'(t)}{|\theta'(t)|} \quad \dots \text{for } |\theta'(t)| \geq \theta_c \\ &= 0 \quad \dots \text{for } |\theta'(t)| < \theta_c\end{aligned}\quad (15)$$

The bed-shear stress (or Shields parameter) is again based on the skin friction part (θ') of the total bed-shear stress, i.e., the form drag induced by bedforms is neglected. For waves, the instantaneous Shields parameter (during the wave cycle) is written as:

$$\theta'(t) = \frac{\frac{1}{2} \rho f'_w |u_b(t)| u_b(t)}{(\rho_s - \rho) g D_{50}} \quad (16)$$

with: $u_b(t)$ = the time-dependent horizontal orbital velocity near the bed at $z = \delta$ (directly above the wave boundary layer).

The wave friction factor f'_w is calculated with the following formula of Swart (1974), which is based on an implicit relation of Jonsson (1966):

$$\begin{aligned}f'_w &= \exp \left(5.2 \left(\frac{k_s}{\hat{a}} \right)^{0.194} - 5.98 \right) \quad \text{for: } \frac{k_s}{\hat{a}} < 0.63 \\ f'_w &= 0.3 \quad \dots \text{for: } \frac{k_s}{\hat{a}} \geq 0.63\end{aligned}\quad (17)$$

Herein: \hat{a} = amplitude of the horizontal near-bed orbital flow.

For the roughness height k_s , a constant representative value is used during the wave cycle, which is calculated with Eq. (13) as follows:

$$k_s = \max \{ 3D_{90}, D_{50} [1 + 6(\langle |\theta| \rangle - 1)] \} \quad (18)$$

in which $\langle |\theta| \rangle$ = time-averaged absolute value or magnitude of the Shields parameter during the wave cycle

$$\begin{aligned}\langle |\theta| \rangle &= \frac{\langle |\tau_b(t)| \rangle}{(\rho_s - \rho) g D_{50}} \\ \langle |\tau_b(t)| \rangle &= \frac{1}{2} \rho f'_w \langle u_b(t)^2 \rangle = \frac{1}{4} \rho f'_w \hat{U}^2\end{aligned}$$

\hat{U} = velocity amplitude of the (sinusoidal) oscillatory flow.

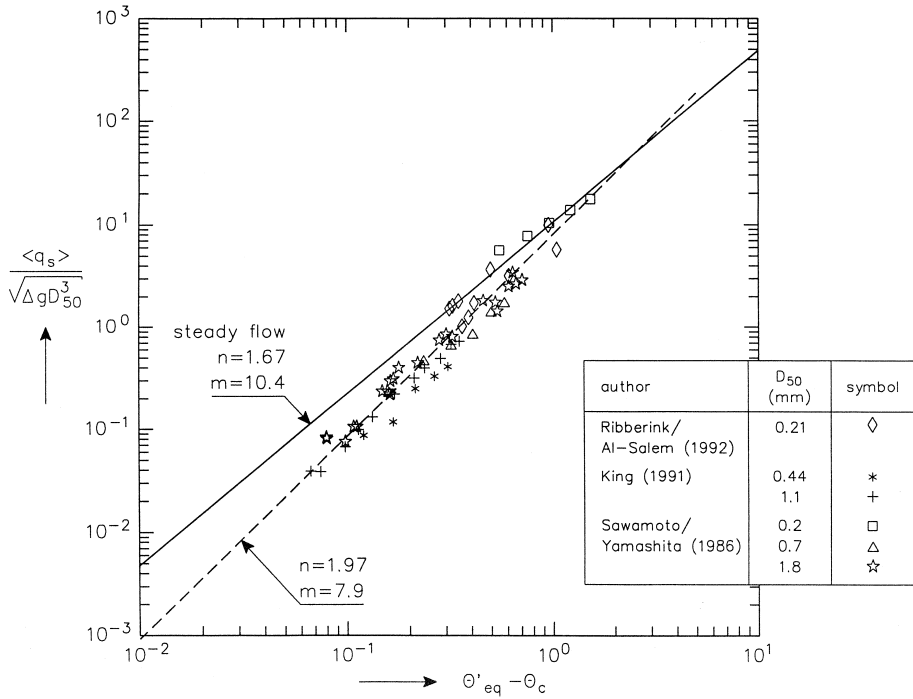


Fig. 5. Oscillatory flows: measured dimensionless net sand transport rates vs. the effective Shields parameter (equivalent value) minus the critical Shields parameter (excess bed-shear), a fitted power formula (dashed line) and the power formula for steady flows (solid line).

Because the available experimental datasets consist of half-cycle and full-cycle transport rate measurements, time-averaging of Eq. (15) is necessary:

$$\langle \Phi_b(t) \rangle = m \left\langle (|\theta'(t)| - \theta_c)^n \cdot \frac{\theta'(t)}{|\theta'(t)|} \right\rangle \quad (19)$$

$\langle \dots \rangle$ = half-cycle (sinusoidal) or full-cycle (2nd-order Stokes) time-averaging.

This formula, together with Eqs. (3), (4), (16)–(18), can be used to compute the net sediment transport rate for oscillatory flows (half-cycle as well as full-cycle averaged). A simple numerical routine is necessary to carry out the time-averaging.

In order to be able to compare the performance of this formula for both the situation of waves and for steady currents, it is useful to characterize the oscillatory flow by an equivalent steady flow, making use of an equivalent Shields parameter θ'_{eq} , which does not vary in time. Its magnitude, $|\theta'_{eq}|$, is related to the absolute magnitude of the net transport rate $|\langle \Phi_b(t) \rangle|$ as follows:

$$|\langle \Phi_b(t) \rangle| = m \{ |\theta'_{eq}| - \theta_c \}^n = m \left\langle \left\{ |\theta'(t)| - \theta_c \right\}^n \cdot \frac{\theta'(t)}{|\theta'(t)|} \right\rangle \quad (20)$$

or:

$$|\theta'_{eq}| - \theta_c = \left(\frac{|\langle \Phi_b(t) \rangle|}{m} \right)^{\frac{1}{n}}$$

(21)

θ'_{eq} represents that value of the Shields parameter, which—in steady flow conditions—would give the same value of the transport rate as Eq. (19) for the oscillatory flow. The magnitude of θ'_{eq} is always greater than the critical Shields value, unless sediment does not come into motion at all during the full wave cycle. Its sign, $\theta'_{eq}/|\theta'_{eq}|$, is equal to that of the calculated net transport rate, $\langle \Phi_b(t) \rangle/|\langle \Phi_b(t) \rangle|$. It should be realized that θ'_{eq} is not a necessary parameter for the net transport computation, it is only defined for comparison purposes of steady and unsteady flows. Its magnitude is always smaller than the maximum (θ'_{max}) and the mean absolute value of the Shields parameter ($\langle |\theta'| \rangle$). In the extreme case of full-cycle averaging of a sinusoidal wave the net transport rate $\langle \Phi_b \rangle$ as well as θ'_{eq} are both equal to zero, despite the large bed shear stresses that may occur during the wave motion.

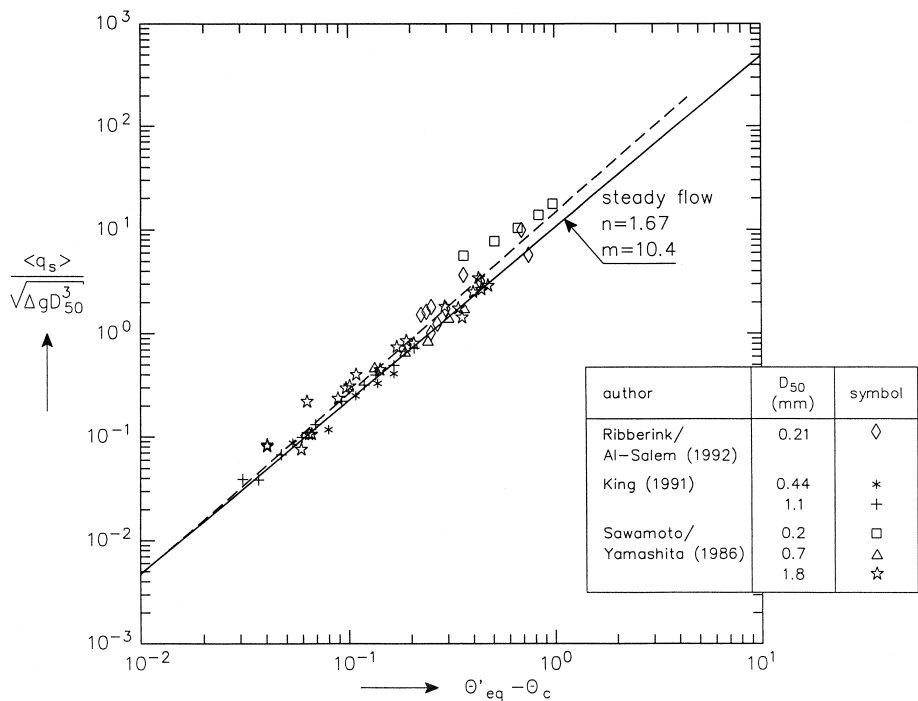


Fig. 6. Oscillatory flows: measured dimensionless net sand transport rates vs. the effective Shields parameter (equivalent value) minus the critical Shields parameter (excess bed-shear), a fitted power formula (dashed line) and the power formula for steady flows (solid line) after adjusting the wave roughness height k_w .

For each individual experiment of the experimental dataset (Table 3), the equivalent Shields parameter θ'_{eq} was determined numerically using Eqs. (20), (16)–(18), (3) and (4). For the power n the value $n = 1.67$, as found from the steady flow experiments, was used (see Eq. (14)).

The measured dimensionless transport rates $\langle \Phi_b \rangle$ are plotted against the computed values of $|\theta'_{eq}| - \theta_c$ in Fig. 5. As for steady flows, the oscillatory flow data also show a good correlation. The scatter of the data can be explained to some extent by the uncertainty introduced during the time-integration process over the wave cycle, which can be considered as a general problem of net sediment transport calculations under the influence of waves.

A power function, fitted through the data points ($m = 7.9$, $n = 1.97$; dashed line in Fig. 5) clearly deviates from the ‘steady flow’ power function ($m = 10.4$, $n = 1.67$; solid line). Especially in the lower Shields regime, the net transport rate for oscillatory flows would be strongly overpredicted with the ‘steady flow’ bed-load formula.

The influence of a slightly increased or decreased value of n on the computed values of θ'_{eq} and on the regression of the oscillatory flow data was then studied but hardly influenced the results and did not lead to an improved agreement with the steady flow

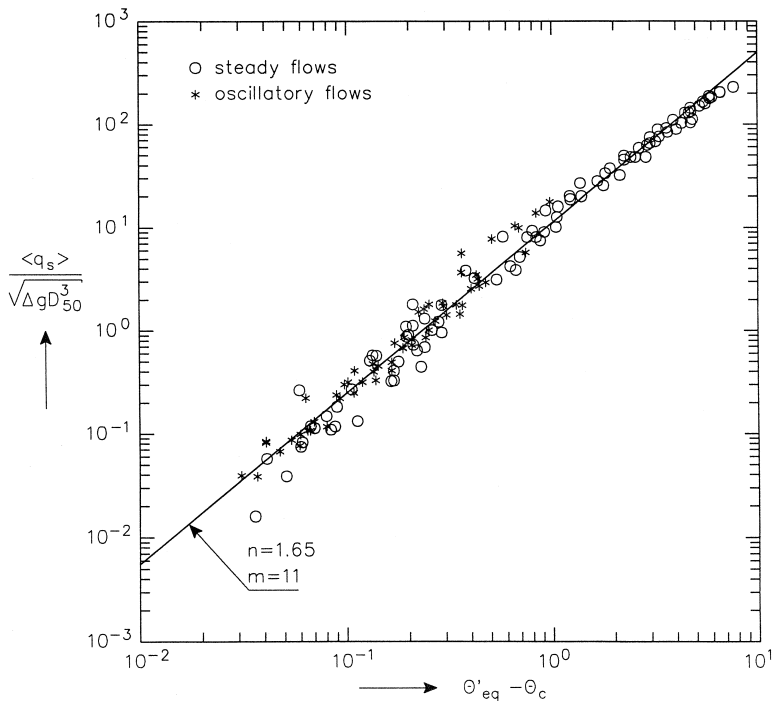


Fig. 7. Steady flows (*) and oscillatory flows (O): measured dimensionless net sand transport rates vs. the effective Shields parameter (equivalent value for oscillatory flows) minus the critical Shields parameter (excess bed-shear) and a fitted power formula for the full data range ($m = 11$, $n = 1.65$).

data. Further study showed that the regression results are strongly influenced by the roughness height k_s . As the modelling of the roughness height was considered to be the most uncertain for oscillatory flows, it was decided to investigate the influence of different options for the lower limit of k_s in Eq. (13) ($k_s = 3D_{90}, 2.5D_{50}, 1D_{50}$). The best result was obtained in the case that k_w is represented by D_{50} (instead of $3D_{90}$) in the low Shields regime. Fig. 6 shows the obtained correlation between $\langle \Phi_b \rangle$ and $|\theta'_{eq}| - \theta_c$ for the same oscillatory flow dataset and in the case that k_w is modelled as:

$$\begin{aligned} k_w &= D_{50} && \text{for: } \langle |\theta| \rangle < 1 \\ k_w &= D_{50} [1 + 6(\langle |\theta| \rangle - 1)] && \text{for: } \langle |\theta| \rangle \geq 1 \end{aligned}$$

(22)

For steady currents k_c is kept unchanged (i.e., $k_c = k_s$ according to Eq. (13)).

It is shown that, due to this separate treatment of the roughness height for oscillatory flows (k_w) and steady flows (k_c), the oscillatory flow data show a much better agreement with the obtained ‘steady flow’ power function ($m = 10.4, n = 1.67$; solid line in Fig. 6). The trend of the oscillatory flow data is shown by the dashed line in Fig. 6. The difference between the two functions is small considering the scatter of the data.

Finally, a new power function was fitted through all data points (steady flows and oscillatory flows). The resulting bed-load formula is shown in Fig. 7 and can be represented by:

$$m = 11, \quad n = 1.65$$

(23)

5. Oscillatory flows with a superimposed current

Experimental studies of bed-load transport in oscillatory flows with a superimposed net current are rather scarce. After the Oscillating Water Tunnel of Delft Hydraulics was extended with a recirculating flow system, a number of sediment transport studies were carried out for various oscillatory flows and superimposed net currents in flat bed

Table 4
Datasets oscillatory flows and superimposed currents

Author	Oscillatory flow	Net current velocity (m/s)	D_{50} (mm)	Number of experiments	Range of θ'_{eq}
Ramadan (1994) (series C1)	2nd-order Stokes	0–0.4 following ^a	0.21	5	0.35–0.75
Ribberink et al. (1994) (series C2)	2nd-order Stokes	0–0.4 following and opposing ^a	0.21	5	0.20–1.10
Katopodi et al. (1994) (series E)	sinusoidal	0.15–0.4	0.21	4	0.75–0.90

^aFollowing = in the direction of the peak/crest velocity of the asymmetric wave.

conditions, using sand with $D_{50} = 0.21$ mm (see Table 4). Ramadan (1994) and Ribberink (1995) combined asymmetric oscillatory flows (2nd-order Stokes waves) with following and opposing net currents of different strengths (series C). Katopodi et al. (1994) conducted detailed experiments, in which sinusoidal waves of increasing velocity amplitudes were combined with net currents of decreasing strength (series E).

The experimental data of the series C and E were analyzed further by Ribberink et al. (1994). They showed that, despite the potential sediment mixing capacity of the flow above the wave boundary layer, in all 14 experiments the total net sediment transport is concentrated in the sheet flow layer and can be considered as bed-load transport. Moreover, the measured net transport rates show a similar linear relation with the third-order moment of the near-bed velocity $\langle u_b^3 \rangle$, as obtained during previous experiments with asymmetric oscillatory flows with no current (see also Fig. 2).

For an oscillatory flow combined with a superimposed current under an arbitrary angle the bed-load model (Eq. (19)) can be written in the following generalized form:

$$\langle \vec{\Phi}_b(t) \rangle = m \left\langle \{ |\theta'(t)| - \theta_c \}^n \cdot \frac{\vec{\theta}'(t)}{|\theta'(t)|} \right\rangle \quad (24)$$

with:

$$|\theta'(t)| = \sqrt{\theta'_x(t)^2 + \theta'_y(t)^2}, \quad m = 11, n = 1.65$$

The subscript x and y refer to the vector components of the (dimensionless) bed-shear stress in a horizontal rectangular x – y plane (see Fig. 8). The instantaneous (intra-wave) bed-load transport and the bed-shear stress have the same direction.

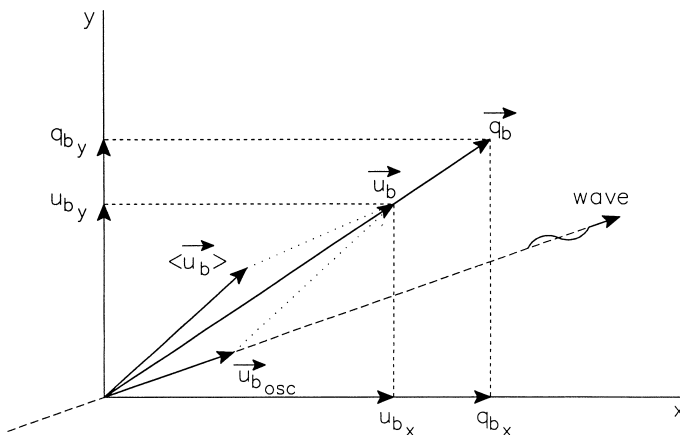


Fig. 8. Definition sketch: vector addition of near-bed velocities due to an oscillatory flow and a superimposed current under an arbitrary angle.

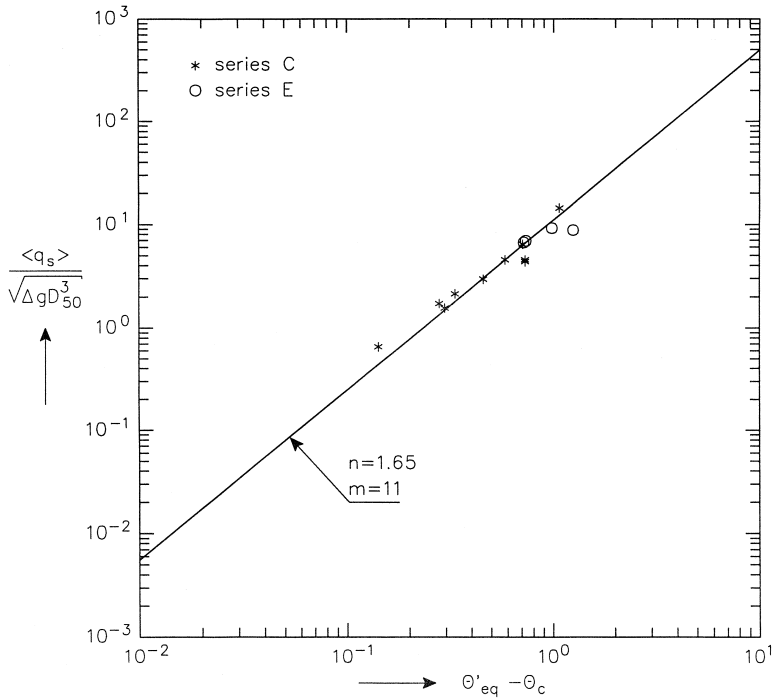


Fig. 9. Oscillatory flows with superimposed currents (co-linear): measured dimensionless net sand transport rates vs. the effective Shields parameter (equivalent value) minus the critical Shields parameter (excess bed-shear) and the power formula ($m = 11$, $n = 1.65$).

The components of the dimensionless bed-shear stress are again calculated with a quadratic friction formula, using the intra-wave near-bed velocities $u_b(t)$ of the combined wave-current motion (at level $z = \delta$) and a wave-current friction factor f'_{cw} :

$$\vec{\theta}'(t) = \frac{\vec{\tau}_b(t)}{(\rho_s - \rho)gD_{50}} = \frac{\frac{1}{2}\rho f'_{cw}|u_b(t)|\vec{u}_b(t)}{(\rho_s - \rho)gD_{50}} \quad (25)$$

$$|u_b(t)| = \sqrt{u_{bx}^2(t) + u_{by}^2(t)}$$

$$\vec{u}_b(t) = \langle \vec{u}_b \rangle + \vec{u}_{b_{osc}}(t)$$

in which: $\langle \vec{u}_b \rangle$ = time-averaged current velocity vector at $z = \delta$; $\vec{u}_{b_{osc}}(t)$ = oscillatory flow velocity vector at $z = \delta$ with magnitude $\hat{U} \sin(2\pi t/T)$ (velocity amplitude \hat{U} and oscillation period T).

Following Madsen and Grant (1976), f'_{cw} is calculated as a linear combination of the wave friction factor f'_w , according to Eq. (16), and a current friction factor f'_c , according to Eq. (10):

$$f'_{cw} = \alpha \cdot f'_c + (1 - \alpha) \cdot f'_w \quad (26)$$

with:

$$\alpha = \langle u_b \rangle / (\langle u_b \rangle + \hat{U})$$

Eqs. (18) and (22) are used for the calculation of the roughness height for respectively the net current (k_c) and for the oscillatory flow (k_w).

For large Shields values both roughness heights become a function of the time-averaged magnitude of the dimensionless bed-shear stress $\langle |\theta'| \rangle$. For combined waves and currents this value is estimated as:

$$\langle |\theta'| \rangle = \frac{\langle |\tau_b| \rangle}{(\rho_s - \rho) g D_{50}} \quad (27)$$

with:

$$\langle |\tau_b| \rangle = 1/2 \rho f'_c \langle u_b \rangle^2 + 1/4 \rho f'_w \hat{U}^2$$

The complete bed-load formula, Eqs. (24)–(27), is verified with the experimental data from Table 4. It should be realized that this dataset is confined to the one-dimensional situation of co-linear oscillatory flows and superimposed currents. The results are presented in Fig. 9, showing the measured values of $\langle \Phi_b \rangle$ as a function of $|\theta'_{eq}| - \theta_c$.

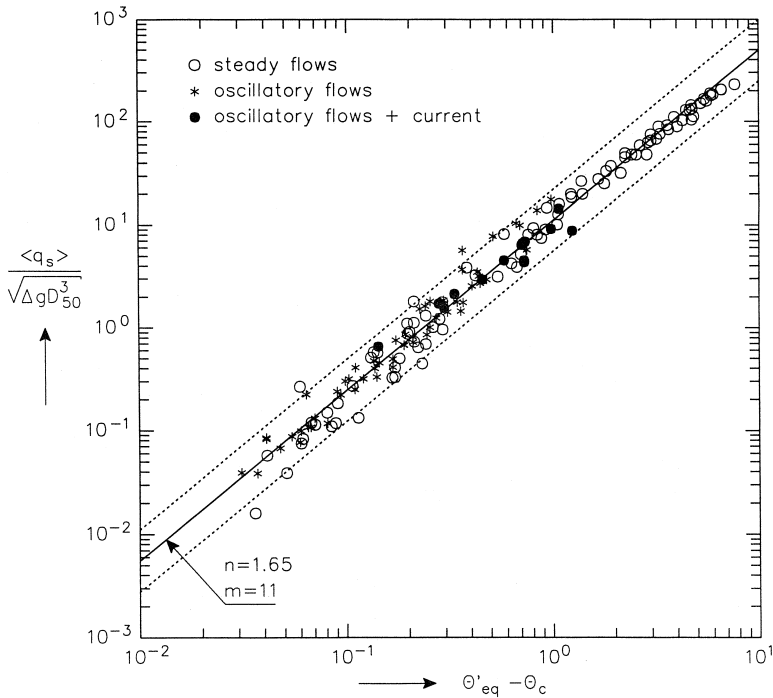


Fig. 10. All steady flow and oscillatory flow data: measured dimensionless net sand transport rates vs. the effective Shields parameter (equivalent value for oscillatory flows) minus the critical Shields parameter (excess bed-shear), the power formula ($m = 11$, $n = 1.65$) and factor 2 deviation ranges.

Table 5

Parameter ranges of the used data

Flow type	θ'_{eq} range	Sediment grain size (mm)	Sediment density (kg/m ³)	Bedforms	Wave period (s)	Wave type
Steady flows	0.07–7	0.2–3.8	2650	dunes + flat bed	—	—
Oscillatory flows	0.1–2	0.2–1.8	2650	flat bed	4–12	R/AS, SINE
Oscillatory + net flow	0.2–1	0.2	2650	flat bed	6.5–7.2	SINE

R = regular waves, AS = asymmetric waves, SINE = sine waves.

The equivalent Shields parameter is determined in the same way as for oscillatory flows with no net current (see Eqs. (20) and (21)). It is shown that the measured bed-load transport rates agree well with the assumed bed-load formula ($m = 11$, $n = 1.65$).

Finally, in Fig. 10, all experimental data are collected in one plot and compared with the obtained bed-load power formula ($m = 11$, $n = 1.65$). Distinction is made between steady flows (open circles), oscillatory flows (stars) and the combined flows (solid circles).

The validity of the formula is limited to bed-load transport of sand and to the conditions of the experimental studies (see Tables 1–4). In Table 5, the main parameter ranges are summarized.

6. Summary and conclusions

The validity of a bed-load transport formula, based on the bed-shear concept of Meyer-Peter and Mueller for steady uniform flows (e.g., river flows), was investigated for steady flows and unsteady oscillatory flow conditions, with the aim to develop a general bed-load transport concept for a wide range of flow and sediment conditions, as occurring in the marine coastal environment. An extensive set of more than 150 laboratory data (steady flows and unsteady oscillatory flows), covering a large range of the Shields parameter (0.07–7), was used for a correlation study between the non-dimensional bed-load transport rate parameter Φ_b and the non-dimensional excess effective bed-shear, as exerted on the sandy bed ($= \theta' - \theta_c$). See Eq. (5) for the general form of the investigated formulation.

As a first step, two complementary sets of bed-load transport measurements in steady flows with and without bedforms (Guy et al., 1966; Nnadi and Wilson, 1992) were used to verify the basic shape of the formula for a large range of Shields values ($0.03 < \theta' - \theta_c < 9$). The data show that, if the power n is fixed at $n = 1.5$, the formula constant m should gradually increase for increasing Shields values. The result of Fernandez Luque and van Beek (1976), $m = 5.7$, is reconfirmed for bed-load data very close to the threshold of motion, Meyer-Peter and Mueller's result, $m = 8$, for the more developed bed-load regime and Wilson's result, $m = 12$, in the sheet flow regime. In the proposed formulation, the effective bed-shear stress, as exerted on the grains, is calculated with a rough-wall friction formulation, using roughness height $k_s = 3D_{90}$ in the lower Shields regime and an implicit relation $k_s = D_{50}(1 + 6(\theta - 1))$, based on the data of Wilson

(1989), in the upper Shields regime with sheet flow. A power-function fit for the full range of Shields values, using all laboratory data and a set of river measurements, resulted in one formula with power $n = 1.67$ and constant $m = 10.4$.

The validity of the obtained formulation was then investigated for unsteady oscillatory flows, assuming that time-history effects or effects of flow unsteadiness during the wave cycle can be neglected (quasi-steadiness). The instantaneous bed-load transport during a wave cycle is then calculated using the bed-load formula and time-averaged in order to obtain net transport rates for half or full wave cycles. A verification was carried out with a set of oscillatory (half-cycle and full-cycle) bed-load measurements with Shields values in the range $0.07 < \theta' - \theta_c < 1.5$ (Sawamoto and Yamashita, 1986; King, 1991; Ribberink and Al-Salem, 1994). By using an equivalent Shields parameter θ'_{eq} , characterizing the bed-shear during the (half or full) wave cycle, the measured net transport rates could be depicted as a function of the excess effective bed shear in the same way as for steady flows. The analysis showed that, especially for low Shields values, the measured unsteady transport rates were systematically overpredicted by the bed-load formula for steady flows. Nevertheless, the experimental data showed a good correlation and could be represented by a similar power function, using adjusted values for the power n ($= 1.97$) and the constant m ($= 7.9$).

Adjustment of the bed-roughness height from $k_s = 3D_{90}$ to $k_s = D_{50}$ (in the lower Shields regime) appeared to have a favourable effect on the results. Especially in the lower Shields regime the excess effective bed-shear reduced and a good agreement was obtained between the steady flow and the unsteady flow data. A power function fit with the complete data set yielded only slightly different values for n ($= 1.65$) and m ($= 11$) than for the steady flow data alone. The physical reasons for this difference in grain roughness for steady flows and unsteady oscillatory flows were not clarified in the present study. They might be attributed to the different character of the bed-load motion in steady flows and unsteady oscillatory flows. In oscillatory sheet flow, grain–grain–flow interactions take place in a considerable part of the wave-boundary layer (sheet flow layer), whereas in steady flows the flow boundary layer generally extends over the full water depth and the sheet flow layer is relatively thin. In addition, it was suggested that an explanation can be found in the fact that the different friction factor formulations for both flow types originate from fixed bed considerations, in which mobile bed effects are not accounted for.

The developed bed-load formulation was generalized for oscillatory flows with a superimposed current under an arbitrary angle. The bed-shear stress was calculated with a quadratic friction law (Jonsson, 1966), using: (i) the horizontal velocity at a prescribed distance from the bed (directly above the wave boundary layer), and (ii) a combined friction factor f_{cw} with different friction factor and roughness height formulations for the net current and the oscillatory current. A verification of this formulation was carried out with a rather limited set of recent bed-load measurements in an oscillating water tunnel with different co-linear oscillatory flow/net current combinations and 0.21 mm sand (Ramadan, 1994; Ribberink, 1995; Katopodi et al., 1994). A good agreement between the computations and measurements was found.

Summarizing, the following uncertainties and restrictions should be mentioned with respect to the validity of the obtained bed-load formula.

(1) In general, the validity of the formula is limited to the parameter ranges of the experimental data as used in this study (see Table 5).

(2) Oscillatory sheet flows with fine sands ($D < 0.2$ mm), light-weight materials and with small wave periods (< 3 s) are excluded from the present analysis, since time-dependent phenomena become important in these conditions and the quasi-steady approach fails (see Janssen and Ribberink, 1996; Janssen et al., 1997).

(3) The formula was not verified for unidirectional free-surface flows in the anti-dune regime and the validity is therefore limited to Froude numbers < 1 and at Shields values (< 1.0).

(4) The formula was verified only for a limited set of co-linear waves and currents and was not verified for oscillatory flows (with or without superimposed net currents) in the regime of fully developed vortex ripples. Especially for regular sinusoidal waves vortex shedding around steep bed ripples leads to an important time-dependent *suspended* transport, which cannot be modelled in a quasi-steady way. Whether the proposed *bed-load* model, including the proposed method for determining θ' , is valid in this type of conditions remains to be seen, and should still be investigated.

Acknowledgements

This publication is the result of research which was mainly undertaken in the framework of the Coastal Genesis research programme in the Netherlands. The author wishes to thank the Ministry of Transport and Public Works in the Netherlands (Rijkswaterstaat, RIKZ) for their important financial support of the experimental programme in the oscillating water tunnel in the period 1992–1995 and for funding the present publication. Thanks are due to the Commission of the European Communities (Directorate General for Science, Research and Development), who also funded part of the research in the framework of the European MAST-G8 Morphodynamics research project. This publication was also made in the framework of the Netherlands Centre of Coastal Research (from Delft Hydraulics and the University of Twente). The author wishes to thank Abdullah Al-Salem, Khaled Ramadan, Irene Katopodi, Ria Koelewijn and Marjolein Janssen who all contributed to parts of the experimental work in the oscillating water tunnel. Special thanks are due to Teun van Maar and Henk Westhuis for their technical assistance. David King is acknowledged for providing the important dataset from the oscillating water tunnel of Scripps. Finally, the author wants to thank Leo van Rijn for his stimulating support during the study and for his useful comments on the draft of this publication.

References

- Al-Salem, A.A., 1993. Sediment transport in oscillatory boundary layers under sheet flow conditions. PhD Thesis, Delft University of Technology.
- Asano, T., 1990. Two-phase model on oscillatory sheet flow. Proc. 22nd Int. Conf. on Coast. Eng., Delft, pp. 2372–2384.

- Bagnold, R.A., 1956. The flow of cohesionless grains in fluids. *Philos. Trans. R. Soc. London, Ser. A* 249, 235–297.
- Bagnold, R.A., 1963. Mechanics of marine sedimentation. In: Hill, M.N. (Ed.), *The Sea*, Vol. 3. Interscience, New York.
- Bailard, J.A., 1981. An energetics total load model for a plane sloping beach. *J. Geophys. Res.* 86 (C11), 10938–10954.
- Bailard, J.A., Inman, D.L., 1981. An energetics bed-load model for a plane sloping beach: local transport. *J. Geophys. Res.* 86 (C3), 2035–2043.
- Bakker, W.T., 1974. Sand concentration in oscillatory flow. *Proc. 14th Int. Conf. on Coast. Eng. and Copenhagen*, pp. 1129–1148.
- Bijker, E.W., 1967. Some considerations about scales for coastal models with movable bed, *Doct. Thesis*, Delft University of Technology.
- Davies, A.G., 1990. Modelling of the vertical distribution of suspended sediment in combined wave-current flow. *Proc. 5th Int. Conf. on the Physics of Estuaries and Coastal Seas*, Gregynog, Univ. of Wales.
- Davies, A.G., Ribberink, J.S., Temperville, A., Zyserman, J.A., 1996. Comparisons between sediment transport models and observations made in wave and current flows above plane beds (submitted for publication in *Coastal Engineering*).
- Dick, J.E., Sleath, J.F.A., 1992. Sediment transport in oscillatory sheet flow. *J. Geophys. Res.* 97 (C4), 5745–5758.
- Einstein, H.A., 1950. The bed-load function for sediment transportation in open-channel flows. *US Soil Conservation Service, Tech. Bulletin No. 1025*, September.
- Engelund, F., Hansen, E., 1967. *A Monograph on Sediment Transport in Alluvial Streams*. Teknisk Vorlag, Copenhagen.
- Fernandez Luque, R., van Beek, R., 1976. Erosion and transport of bed-load sediment. *J. Hydr. Res. IAHR* 14 (2), 127–144.
- Fredsoe, J., Andersen, O.H., Silberg, S., 1985. Distribution of suspended sediment in large waves. *J. Waterway Port Coastal Ocean Eng. ASCE* 111 (6), 1041–1059.
- Guy, H.P., Simons, D.B., Richardson, E.V., 1966. Summary of alluvial channel data from flume experiments, 1956–1961. *US Geological Survey, Prof. Paper 462-I*, Washington, DC.
- Hansen, E.A., Fredsoe, J., Deigaard, R., 1994. Distribution of suspended sediment over wave-generated ripples. *J. Waterway Port Coast. Ocean Eng. ASCE* 120 (1), 37–55.
- Horikawa, K., Watanabe, A., Katori, S., 1982. A laboratory study on suspended sediment due to wave action. *Proc. 18th Int. Conf. Coast. Eng., ASCE, Cape Town*.
- Janssen, C.M., Ribberink, J.S., 1996. Grain-size influence on sand transport in oscillatory sheet flow. *Proc. 25 Int. Conf. on Coast. Eng., ASCE, Orlando, USA*, pp. 4779–4792.
- Janssen, C.M., Hassan, W.H., van der Wal, R., Ribberink, J.S., 1997. Grain-size influence on sand transport mechanisms. Paper presented during *Coastal Dynamics '97*, Plymouth, June.
- Jonsson, I.G., 1966. Wave boundary layers and friction factors. *Proc. 10th Int. Conf. on Coast. Eng.*, pp. 127–148.
- Katopodi, I., Ribberink, J.S., Ruol, P., Koelewijn, R., Lodahl, C., Longo, S., Crosato, A., Wallace, H., 1994. Intra-wave sediment transport in an oscillatory flow superimposed on a mean current. *Delft Hydraulics, Data report H1684, Part III (MAST-G8M)*.
- King, D.B., 1991. *Studies in oscillatory flow bedload sediment transport*. PhD Thesis, Univ. of California, San Diego.
- Madsen, O.S., Grant, W.D., 1976. *Sediment transport in the coastal environment*. MIT Ralph M. Parsons Lab., Rep. 209, Cambridge, USA.
- Meyer-Peter, E., Mueller, R., 1948. Formulas for bed-load transport. *Proc. IAHR, Stockholm*, 1948.
- Nnadi, F.N., Wilson, K.C., 1992. Motion of contact-load particles at high shear stress. *J. Hydr. Eng. ASCE* 118 (12).
- Ramadan, K.A.H., 1994. Time-averaged sediment transport phenomena in combined wave-current flows. *MSc. Thesis, IHE Delft, Delft Hydraulics, Report H1889.11, Part I*, January.
- Ribberink, J.S., 1995. Time-averaged sediment transport phenomena in combined wave-current flows. *Delft Hydraulics, Report H1889.11, Part II*, March.

- Ribberink, J.S., Chen, Z.W., 1993. Sediment transport of fine sand under asymmetric oscillatory flow. Delft Hydraulics, Report H840, Part VII, January.
- Ribberink and Al-Salem, 1992.
- Ribberink, J.S., Al-Salem, A.A., 1994. Sediment transport in oscillatory boundary layers in cases of rippled bed and sheet flow. *J. Geophys. Res.* 99 (C6), 12707–12727.
- Ribberink, J.S., Al-Salem, A.A., 1995. Sheet flow and suspension in oscillatory boundary layers. *Coast. Eng.* 25, 205–225. (See also: Ribberink and Al-Salem, 1992 and Al-Salem, 1993).
- Ribberink, J.S., Katopodi, I., Ramadan, K.A.H., Koelewijn, R., Longo, S., 1994. Sediment transport under (non)-linear waves and currents. *Proc. 24th Int. Conf. on Coast. Eng.*, ASCE, Kobe, Japan.
- Sato, S., 1987. Oscillatory boundary layer flow and movement over ripples. PhD Thesis, Univ. of Tokyo, 135 pp.
- Sawamoto, M., Yamashita, T., 1986. Sediment transport rate due to wave action. *J. Hydrosc. Hydr. Eng.* 4 (1), 1–15.
- Smith, J.D., 1977. Modelling of sediment transport on continental shelves. In: *The Sea*, Vol. 6. Wiley-Interscience, New York, pp. 539–577.
- Staub, C., Jonsson, I.G., Svendsen, I.A., 1984. Variation of sediment suspension in oscillatory flow. *Proc. 19th Int. Conf. Coast Eng.*, Houston, pp. 2310–2321.
- Swart, D.H., 1974. Offshore sediment transport and equilibrium beach profiles. Delft Hydr. Lab. Publ., No. 131, Delft Hydraulics, The Netherlands.
- van den Berg, J.H., 1986. Aspects of sediment and morphodynamics of subtidal deposits of the Oosterschelde (the Netherlands), Rijkswaterstaat, Communications no. 43.
- van Rijn, L.C., 1981. Entrainment of fine sediment particles, computation of bed-load concentration and bed-load transport. Delft Hydraulics, Report S487, Part I.
- van Rijn, L.C., 1982. Equivalent roughness of alluvial beds. *J. Hydr. Div. ASCE* 108 (HY 10).
- van Rijn, L.C., 1993. Principles of sediment transport in rivers, estuaries and coastal seas. Aqua Publications, Amsterdam, The Netherlands.
- Villaret, C., Perrier, G., 1992. Transport of fine sand by combined waves and current: an experimental study. *Electricité de France Report No. HE-42/92.68*, 81 pp.
- Wilson, K.C., 1966. Bed-load transport at high shear stress. *J. Hydr. Div. ASCE* 92 (HY 6), 49–59.
- Wilson, K.C., 1987. Analysis of bed-load motion at high shear stress. *J. Hydr. Div. ASCE* 113 (1), 97–103.
- Wilson, K.C., 1989. Friction of wave-induced sheet flow. *Coast. Eng.* 12, 371–379.